

EFFICIENT CAD OF E-PLANE STEPS IN RECTANGULAR WAVEGUIDE

M. Mongiardo† and T. Rozzi*

†Dipartimento di Ingegneria Elettronica, Università di Roma, 'Tor Vergata', Rome, Italy.

*Dipartimento di Elettronica e Automatica, Università di Ancona, Italy,
and Department of Electrical Engineering, University of Bath, UK.

ABSTRACT

Cascaded E-plane steps in waveguide still find a variety of uses in microwave components for power applications and in millimetres.

Wideband synthesis requires efficient field analysis, leading to simple equivalent circuits with frequency independent elements, so as to avoid repeating the field analysis at each frequency.

We present the results of an analytical approach in a form suitable for CAD on a desktop computer.

INTRODUCTION

The widely used modal analysis of waveguide step discontinuities employs the eigenmode of the guiding structures to represent the field on the discontinuities. Unfortunately, even if the eigenmodes form a complete basis, their use is particularly inefficient when field singularities due to the edges are present. On the other hand, in these cases other bases can be used that represent the fields well. By using the latter bases, it is possible to obtain very accurate determination of the parameters of the discontinuity (e.g. the reflection coefficient or the admittance) even using a single basis function. If, in addition, lumped models are provided for the modal admittance, then simple, wide-band, equivalent circuits can be derived. Since these circuits contain frequency independent elements only, they can be efficiently used in CAD.

ANALYSIS

When an electromagnetic field impinges on the discontinuity of Figure 1 higher order modes are excited in order to satisfy the boundary conditions. However, if the incident mode has no electric field component in the x-direction, only LSE modes are generated. These modes can be derived from an x-directed magnetic vector potential. Standard textbook analysis provides the expressions for the field components transverse to the discontinuity. In the following we assume, with respect to Fig. 1, that p modes can be incident on the discontinuity from the left, and that p' modes can be incident from the right.

By imposing the continuity of the transverse field across the aperture, and by using linearity, we obtain the following integral equations for the electric field E_k

$$Y_k^{1/2} g_k = \hat{Y} E_k \quad (1)$$

where Y_k is the normalised admittance of the mode k incident on the discontinuity, and g_k represents the y dependence of this mode. \hat{Y} is the integral operator whose kernel is the Green's admittance function in the scattering representation and is given by

$$Y(y, \eta) = \frac{1}{2} \sum_{n=0}^{\infty} \left[Y_n \varphi_n(y) \varphi_n(\eta) + Y'_n \varphi'_n(y) \varphi'_n(\eta) \right] \quad (2)$$

where the $\varphi_n(y)$ describe the y-dependence of the modes.

Once E_k is found the scattering matrix is easily computed as

$$S_{ik} = Y_i^{1/2} \langle g_i, E_k \rangle - \delta_{ik} \quad (3)$$

with

$$\delta_{ik} = \begin{cases} 0 & i \neq k \\ 1 & i = k \end{cases}$$

To solve the integral equation (3) by Galerkin method an appropriate, preferably orthonormal, set of expanding functions must be selected. Since the weight function of the Gegenbauer polynomials of order $\nu = 1/6$ satisfy the 90° corner edge condition, these weighted polynomials can be successfully chosen as the expansion set. According to the even parity of the field, and taking into account the normalisation factor N_m , the expansion set $\psi_m(y)$ is

$$\psi_m(y) = \frac{1}{\sqrt{b}} \frac{1}{N_m} C_{2m}^{1/6} \left[\frac{y}{b} \right] W(y) \quad m = 0, 1, \dots, N-1 \quad (4)$$

$$W(y) = \left[1 - \left(\frac{y}{b} \right)^2 \right]^{-1/3}$$

and consequently the field E_y is expressed as

$$E_k(y) = \sum_{m=0}^{N-1} \lambda_{km} \psi_m(y) \quad (5)$$

When (5) is used the equations (1) are correspondingly mapped into the matrix equations

$$Y_k^{1/2} \underline{G}_k = \underline{Y} \underline{\Delta}_k \quad (6)$$

where the matrix elements are given by

$$Y_{mk} = \frac{1}{2} \sum_{m=0}^{\infty} \left\{ Y_n P_{mn} P_{kn} + Y'_n P'_{mn} P'_{kn} \right\} \quad (7)$$

and

$$P'_{mn} = \int_0^b \psi_m(y) \varphi_n'(y) dy = \sqrt{2s} C_m \frac{J_{2m+1/6}(n\pi s)}{(n\pi s)^{1/6}}$$

$$C_m = [-1]^m \left[\frac{\pi \Gamma(1/3+2m)}{(2m)!} \right]^{1/2} (2m + 1/6)^{1/2}$$

Equation (6) is numerically invertible and leads via (3) to the sought variational expression for the scattering matrix

$$S_{ik} = Y_i^{1/2} \underline{G}_i^T \underline{Y}^{-1} \underline{G}_k Y_k^{1/2} - \delta_{ik} \quad (8)$$

However, in practice, one is interested in the scattering matrix over a wide frequency band, and this means that one should recalculate the matrix \underline{Y} and its inverse for each frequency point. As will be evident from the next section, the dimensions of matrix \underline{Y} , due to the chosen basis, are very small (i.e. \underline{Y} is 1*1 or at maximum 2*2) and therefore its inversion is a straightforward matter. The time-consuming task in the calculation of (8) is therefore relative to the sum appearing in (7).

The numerical effort of computing (7) can be greatly reduced by taking advantage of the quasi-static approximation for the modes well below cutoff ($n \gg NF1, NF2$)

$$Y'_n = \frac{1}{n} \frac{ju}{\sqrt{1 - (\frac{u}{n})^2}} \approx \frac{ju}{n} \quad n \gg u$$

$$u = \frac{b}{\pi} \sqrt{k_o^2 - (\frac{\pi}{a})^2}$$

where u is the normalised frequency and is such that $u = 0$ at cutoff of the fundamental mode and $u = 1$ at that of the first higher order LSE mode in the larger guide. By using this approximation we obtain

$$Y_{mk} = \frac{1}{2} \left\{ \sum_{n=0}^{NF1-1} Y_n P_{mn} P_{kn} + \sum_{n=0}^{NF2-1} Y'_n P'_{mn} P'_{kn} \right\} + \quad (9)$$

$$+ \frac{ju}{2} \left\{ s \sum_{n=NF1}^{\infty} \frac{1}{n} P_{mn} P_{kn} + \sum_{n=NF2}^{\infty} \frac{1}{n} P'_{mn} P'_{kn} \right\}$$

and while the expression inside the first brackets needs to be recalculated at such frequency, the other expression needs to be calculated just once. Equation (9) still doesn't provide a simple equivalent circuit. This can be obtained by expanding the modal admittances into continuous fractions up to the second order

$$Y'_n = \frac{1}{n} \frac{ju}{\sqrt{1 - (\frac{u}{n})^2}} = \frac{1}{3} \frac{ju}{n} + \frac{2}{3} \frac{ju}{1 - \frac{3}{4} \frac{u^2}{n^2}}$$

Consequently $Y_n(u)$ can be represented to a high degree of approximation by the lumped frequency independent LC-ring of Fig. 2b. We are now in a position to draw an entire class of equivalent circuits depending on the different values of $NF1$ and $NF2$ retained, and to the number of basis functions considered.

RESULTS

An extensive numerical analysis has been carried out in order to ascertain the convergence of the basis function set chosen to express the electric field in the aperture. In table 1 the modulus of the reflection coefficient has been calculated by using 1,...,4 basis functions incorporating the 90° edge condition. These data have been compared with the previous results obtained by Rozzi^[1] using 2 basis functions of the type used by Schwinger. Apart from noting the excellent agreement, it is also possible to verify that two basis functions always provide stable results, and that even the first order approximation (one basis function only) gives very accurate values. This is further confirmed by the results of table II.

By using the theory developed in section 2 it is therefore possible to design very accurate and simple equivalent circuits. For example, if only the fundamental mode is propagating at either side of the discontinuity and if we retain the dynamical behaviour of the first higher order modes on each side, we obtain the equivalent circuit of Fig. 3. This equivalent circuit can then be used to model cascaded discontinuities. An example in this sense is provided by Fig. 4, that compares the experimental results obtained by Bosma (dots)^[2] with the numerical results (obtained using only one basis function) in the cases of thick (continuous curve) and thin (dotted line) iris. The importance of taking into account the finite thickness of the iris discontinuity is evident.

CONCLUSIONS

The classical problem of coupled E-plane step discontinuities has been reconsidered. It has been shown that including the edge condition it is possible to find a basis that, with only one or at maximum two terms, represents, to a high degree of precision, the field aperture. The frequency dependence of the problem has been considered and simplified by assuming the equivalent lumped representation of the modal admittances. As a result a simple, broad-band, equivalent circuit has been given that provides an efficient tool for CAD analysis of cascaded discontinuities.

REFERENCES

[1] T.E. Rozzi, "A new approach to the network modelling of capacitive irises and steps in waveguides", Int. J. Circuit Theory Appl. vol. 3, pp 339-354, Dec. 1975.

[2] H. Bosma, "Two capacitive windows in a rectangular waveguide", Appl. Sci. Res., vol. B7, pp 131-144, 1959.

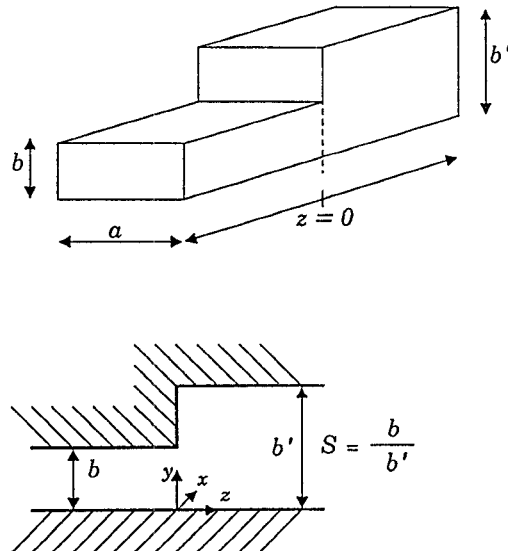


Fig. 1 Geometry of the single E-plane step

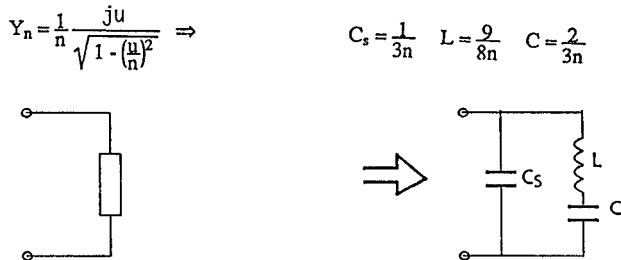


Fig. 2 Equivalent circuit of the modal admittance

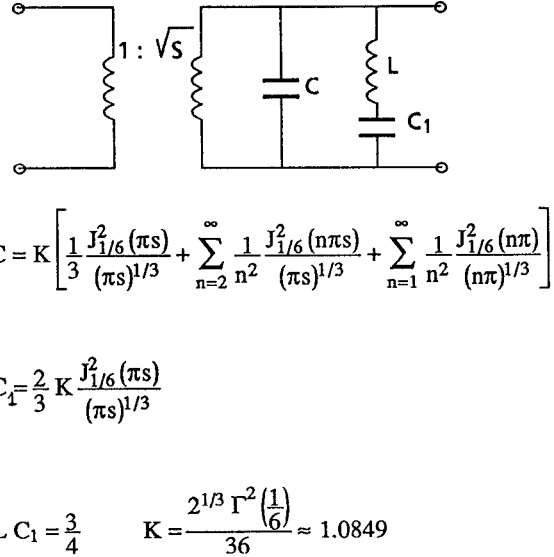


Fig. 3 Equivalent circuit corresponding to the one-term approximation.

s	NY	1	2	3	4	Ref. [1]
0.2		.6794	.6793	.6793	.6793	.6791
0.4		.4483	.4479	.4479	.4479	.4478
0.6		.2631	.2620	.2619	.2619	.2622
0.8		.1170	.1140	.1139	.1139	.1143

TABLE I

The modulus of the reflection coefficient reported in columns, 1,...,4 is obtained using respectively 1,2,...,4, basis function to represent the field on the aperture. The results in column 5 are taken from [1] where two basis functions were used.

NY	1	2	3	4
0.2	.6732	.6731	.6731	.6731
0.8	.1142	.1126	.1126	.1126

a) $F = 8$ GHz

NY	1	2	3	4
0.2	.7091	.7090	.7090	.7090
0.8	.1283	.1205	.1204	.1204

b) $F = 12$ GHz

TABLE II

Modulus of the reflection coefficient for two different heights of the step ($s = 0.2, 0.8$) and two values of frequency for a standard X-band waveguide. NY represents the number of basis functions used to approximate the field on the aperture.

MODULUS TRANSMISSION COEFFICIENT

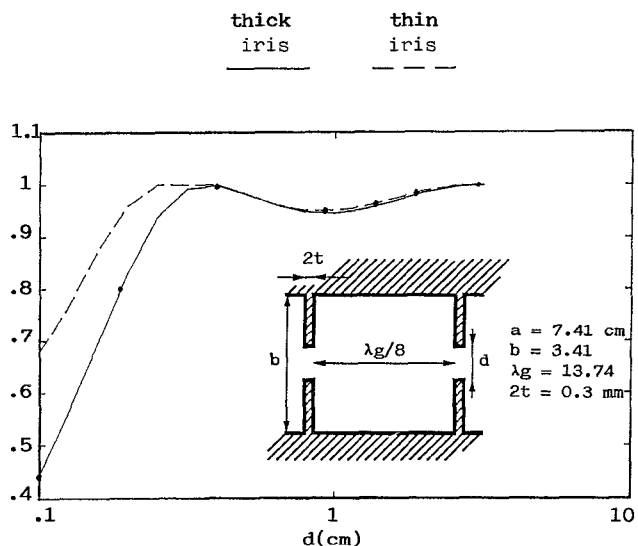


Fig. 4 Comparison of the experimental results of [2] with our numerical simulation. The geometry of the discontinuity is shown in the inset.